Thermal Behavior and Kinetics During the Stabilization of Polyacrylonitrile Precursor in Inert Gas

Shijie Xiao,[1,2] Honghong Lv,[1] Yuanjian Tong,[1] Lianghua Xu,[1] Biaohua Chen[2]

[1]*National Carbon Fiber Engineering Research Center, Beijing University of Chemical Technology, Beijing 100029, China*
[2]*State Key Laboratory of Chemical Resource Engineering, Beijing University of Chemical Technology, Beijing 100029, China*

Received 25 May 2010; accepted 26 October 2010
DOI 10.1002/app.33656
Published online 27 April 2011 in Wiley Online Library (wileyonlinelibrary.com).

ABSTRACT: The thermal behaviors of polyacrylonitrile precursor during thermal stabilization in inert gas were investigated by differential scanning calorimetry, thermomechanical analysis, and thermogravimetry. Combining these methods with the tracing of chemical changes by Fourier transform infrared spectroscopy indicated that complex reactions, including cyclization and pyrolytic reactions occurred sequentially. An imine-enamine tautomeric structure was formed at around 240°C and was converted to a conjugated structure when the temperature was increased to 400°C. A thermal stabilization mechanism was proposed and confirmed experimentally by using a two-step heating process. The apparent activation energies and the pre-exponential factors for these stabilization reactions were also estimated by the Kissinger, Ozawa, and "Improved Coats-Redfern" methods. To obtain a fit to the experiment data, a new kinetic model, named the "Three Regions Kinetic Model," was proposed using the Improved Coats-Redfern method. The applicability of this model and the prediction of the stabilization profile at a given heating rate were verified by plotting conversion rate against conversion profiles. © 2011 Wiley Periodicals, Inc. J Appl Polym Sci 122: 480–488, 2011

Key words: polyacrylonitrile; stabilization; thermal behavior; kinetics

INTRODUCTION

Polyacrylonitrile (PAN) fibers are widely used as precursors for fabricating high performance carbon fibers. During the production of carbon fiber, one of the key processes is the so-called thermal stabilization process, during which PAN fibers are converted to infusible, nonflammable fibers by heating to 200–300°C for about 1 h. During this process, complex chemical reactions occur, accompanied by significant enthalpy changes and thermal shrinkage. Since the 1950s, various kinds of reaction schemes have been proposed to interpret the phenomena that take place during thermal stabilization.[1–9] In an inert atmosphere, cyclization of the PAN molecular chains and the liberation of micromolecular gases take place. In air, the situation becomes much more complicated due to the presence of oxygen.

Thermal analysis methods are frequently employed for investigating cyclization kinetics which are useful to follow the transitions that occur during thermal stabilization. For instance, Fitzer and Muller[10] compared the cyclization rate of PAN homopolymer and copolymer fibers in N_2 and air by differential thermal analysis (DTA) and concluded that the cyclization followed first order kinetics. Differential scanning calorimetry (DSC) has also been employed by other researchers.[8–14] For example, Collins et al.[11] investigated cyclization kinetics in air and proposed a dual consecutive first-order kinetic model to describe the data. However, to our knowledge, normally only single thermal analysis methods have been applied to the investigation of stabilization kinetics in the literatures. Because of the complexity of the thermal stabilization process, a combination of several thermal analysis methods could be beneficial for clarifying the thermal stabilization mechanism.

To clarify the kinetic characteristics of thermal stabilization, the cyclization reaction has been investigated by various mathematical methods in the past. The Kissinger[15] and Ozawa[16] methods are the major kinetic methods that involve plotting the DSC peak temperatures at different heating rates. A simple nth-order fitting model using Fourier transform infrared spectroscopy (FT-IR) has also frequently been used.[17,18] In addition, other models, such as the nth-order autocatalytic model, based on isothermal DSC curves, have also been reported.[13] In our study, based on distinguishing between several simultaneous reactions occurring at

Correspondence to: L. Xu (xulh@mail.buct.edu.cn).
Contract grant sponsor: National Basic Research Program of China; contract grant number: 2006CB605302.

sufficiently high temperatures, multiple kinetic models are used to evaluate the different steps of this complicated reaction process. The Improved Coats-Redfern method based on DSC curves was used to generate insight into the cyclization kinetics.

EXPERIMENTAL

Materials

A commercial PAN fiber sample containing a small amount of itaconic acid and methacrylate comonomers was obtained and used for DSC, TMA, TG, and FT-IR measurements.

Measurements

Differential scanning calorimetry

The enthalpy change of PAN short fibers during the heating process was investigated using a TA instrument DSC Q100 from 40 to 400°C under N_2 atmosphere at heating rates that varied from 2 to 10°C min^{-1}. The sample size for the measurements was about 3 mg. The gas flow rate was 50 mL min^{-1}.

Thermomechanical analysis

The thermal shrinkage of PAN fibers was obtained by a TA instrument TMA Q400. The samples were scanned during the heating process from 40 to 400°C at various heating rates from 2 to 10°C min^{-1} under N_2 atmosphere. The tension applied to the fibers was extremely small so that the fibers could shrink freely. The gas flow rate was 100 mL min^{-1}.

Thermogravimetry

The mass loss of PAN short fibers was investigated using a Netzsch STA449C instrument. About 5 mg of samples were evenly dispersed in an Al_2O_3 pan and scanned at various heating rates from 2 to 10°C min^{-1} under Ar atmosphere between 40 and 400°C. The gas flow rate was 24 mL min^{-1}.

Fourier transform infrared spectroscopy

Infrared spectral measurements were performed using a Nicolet 5700 instrument. KBr disks were prepared by mixing KBr and sample powder homogeneously.

Two-step heating process

The PAN samples were heated from 40 to 240°C at 2°C min^{-1} heating rate under N_2 atmosphere, then held isothermally for 2 h. This process was identified as A. After cooling to 40°C, the samples were heated again to 400°C at 10°C min^{-1} under N_2 atmosphere. This process was identified as B. The thermal behaviors of PAN fibers during both A and B processes were traced by DSC and TMA. The samples at different stages were weighed by electronic balance and measured by the FT-IR instrument.

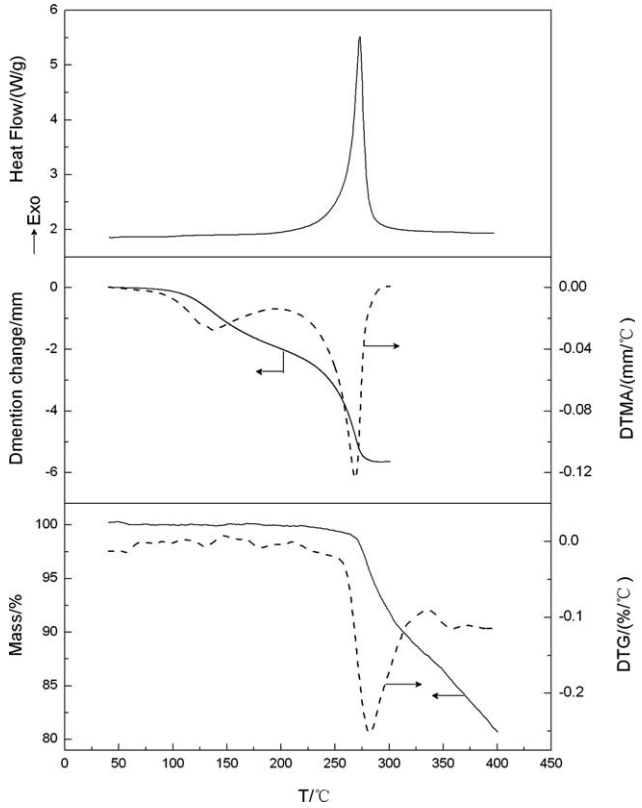

Figure 1 Thermal behavior curves of PAN fibers in inert gas (β = 6°C min^{-1}).

RESULTS AND DISCUSSION

Thermal analysis

Thermal behaviors of PAN fibers during the heating process in N_2 atmosphere were compared by DSC, TMA, and TG methods. The results are shown in Figure 1. The three curves show some correlation during the thermal stabilization process. The sharp single exothermic peak at around 273°C observed from the DSC curve can be attributed to the cyclization of PAN molecular chains. Two steps of shrinkage can be observed from the TMA and DTMA (first order differential of TMA) data, including physical shrinkage caused by the release of inner physical stress at around 135°C and chemical shrinkage that result from cyclization at around 268°C, which is close to the exothermic peak in the DSC curve. The TG results indicate that the mass loss caused by pyrolytic reactions mainly occurred when the temperature was higher than 263°C.

By analyzing the results in detail, the characteristic parameters of the thermal behaviors are listed in Table I, where T_i is the initial temperature, T_p is the peak temperature, and T_f is the final temperature

TABLE I
Characteristic Parameters in Figure 1

Methods	T_i (°C)	T_p (°C)	T_f (°C)
DSC	216	273	307
TMA	224	268	284
TG	263	282	–

[T_p was obtained by DTMA and DTG (first order differential of TG)]. By comparing these results we can observe that: (a) T_i(DSC) < T_i(TMA) < T_i(TG), where T_i(TG) is ~ 47°C higher than T_i(DSC) and about 39°C higher than T_i(TMA); (b) the order of T_p is T_p(TMA) < T_p(DSC) < T_p(TG); (c) when the temperature is higher than T_f(DSC) and T_f(TMA), PAN fibers still continue to lose weight. Similar results were also acquired by analyzing the thermal behavior curves of PAN under different heating rates. These results imply that complex reactions occur in PAN fibers at temperatures from 200 to 350°C in inert gas.

Based on the above analysis of the thermal behaviors, especially the sequence of T_i and T_p, a mechanism for thermal stabilization of PAN fibers can be deduced as follows. At first, disorientation of the molecular chains occurs and leads to physical shrinkage of the PAN fibers from the macro-viewpoint. With an increase in heat treatment temperature, cyclization of nitrile groups occurs, leading to intensive enthalpy change and significant shrinkage of PAN fibers. Furthermore, when the temperature is sufficient, pyrolytic reactions take place, which results in mass loss of PAN fibers. Meanwhile, cyclization reactions proceed until the residual nitrile groups become difficult to react with other functional groups. The pyrolytic reactions of PAN fibers then continue with little heating and shrinking effects.

The overlapping of the wide temperature regions of cyclization and pyrolytic reactions make it difficult to clarify the overall evolution during the heating process. To separate the cyclization reaction from pyrolytic reactions and to demonstrate the mechanism proposed above, a two-step heating process described in the experimental section was designed and carried out in DSC, TMA, and TG instruments. The initial temperatures obtained from DSC and TG were plotted against the heating rate. The results are shown in Figure 2(a,b) respectively, from which we estimated the extrapolated temperature values of the DSC and TG curves as 193 and 248°C, respectively, (the extrapolated initial temperature was acquired from the crossover point of the curve and *Y*-axis). This indicates that the cyclization occurs above 193°C and pyrolytic reactions take place above 248°C. A temperature at 240°C was selected as the isothermal temperature for the first heating process so that the cyclization proceeded as far as possible, whereas pyrolytic reactions would not occur. Figure 3 shows the DSC and TMA results of PAN fibers undergoing the two-step heating process. Comparisons of the change of enthalpy (ΔH), chemical shrinkage (ΔL), and mass loss (ΔM) of PAN fibers between the two heating steps are shown in Table II. The data shows a significant difference between the two heating steps. During the first heating step, ΔH and ΔL were more marked than during the second heating step, but the mass loss was much lower. This indicates that cyclization was the principal reaction during the first heating step. The mass loss in the first step may be attributed to the cyclization reaction because micromolecular gases such as HCN, H_2O, and H_2 could have escaped from PAN due to the cyclization. The dominant reactions during the second heating step were the pyrolysis of PAN fibers, which resulted in a much higher relative mass loss. A relatively small amount of enthalpy change and chemical shrinkage was still generated during this step, which may be attributed to the further cyclization of PAN molecular chains, which occurred at the same time

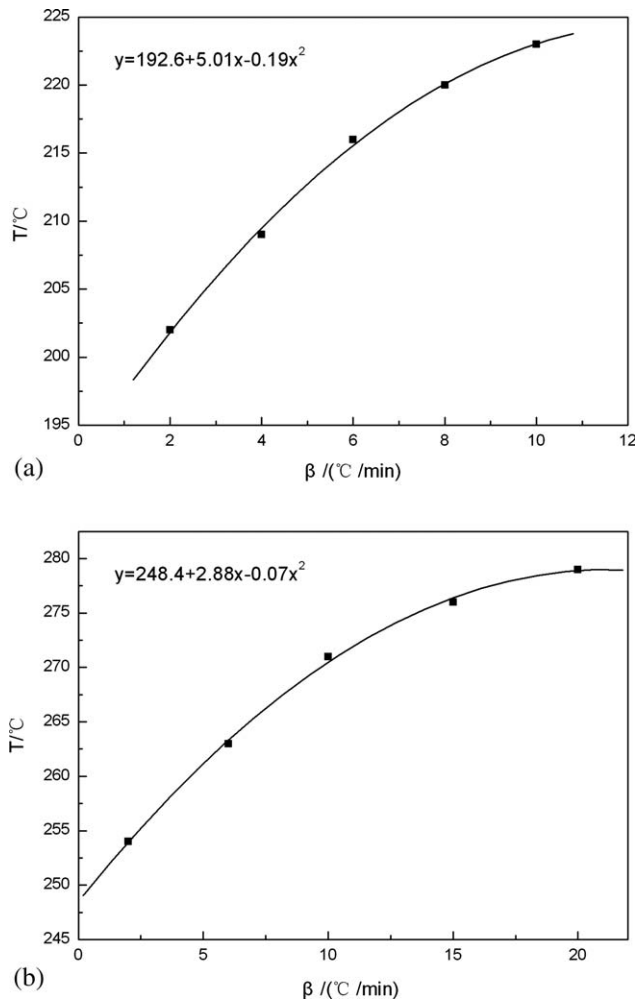

Figure 2 Extrapolated curves of initiation temperature of PAN fibers by (a) DSC; (b) TG curves.

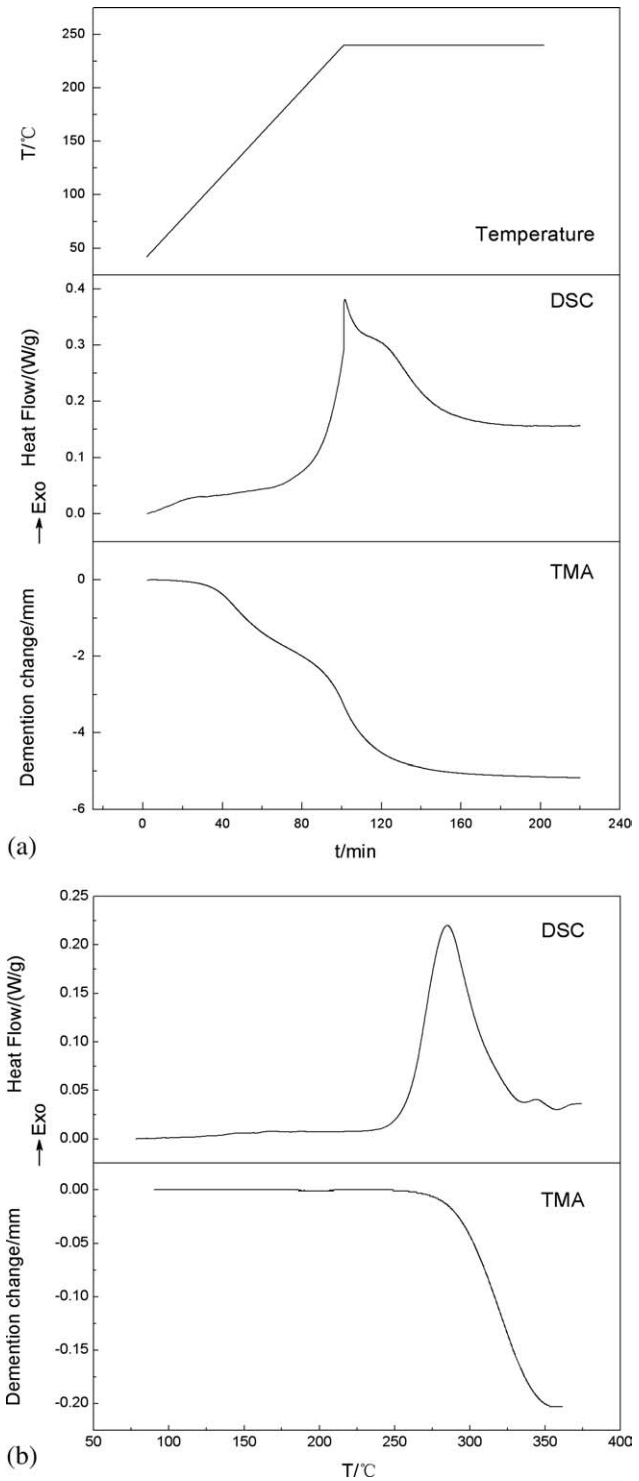

Figure 3 Thermal behavior curves of PAN fibers: (a) First heating process; (b) Second heating process.

as pyrolytic reactions. Definitive reaction mechanisms during this stage are unclear.

FT-IR analysis

Figure 4 shows the heat-treatment dependence in the FT-IR spectra of PAN fibers during the two-step heating processes. Figure 4(a) shows the spectrum for the PAN precursor. There is a strong absorption band at 2243 cm^{-1} assigned to the $\nu_{C\equiv N}$ band (the stretching mode of the nitrile group). The assignments of other significant absorption bands are as follows[2,19]: the band at 2940 cm^{-1} is assigned to the ν_{C-H} band of methylene, the band at 1454 cm^{-1} is assigned to the δ_{C-H} band (the bending vibration of C—H) of methylene, and the band at 1736 cm^{-1} is assigned to the $\nu_{C=O}$ band of carboxy. As shown in Figure 4(b), after the first heating process, all of these characteristic bands of the PAN precursor decreased, while two new bands at 1615 and 1575 cm^{-1} can be observed, which are assigned to $\nu_{C=N}$ and $\nu_{C=C}$, respectively. Kakida and Tashiro[20] suggested that under N_2 gas the stabilized structure does not conjugate fully. The Imine-enamine tautomerism results in the splitting of the 1615 cm^{-1} ($\nu_{C=N}$) and 1575 cm^{-1} ($\nu_{C=C}$) bands. This is illustrated in Figure 5. The fraction of unreacted nitrile groups was also calculated to evaluate the development of cyclization according to the expression deduced by Collins et al.[11] as shown below:

$$f = \frac{I_{C\equiv N}}{I_{C\equiv N} + 0.29 I_{C=N}} \quad (1)$$

where f represents the fraction of unreacted nitrile groups and I is the measured absorption intensity. The value of f after the first heating process [Fig. 4(b)]

TABLE II
Contrast of the Two-Step Heating Processes in Figure 3

Process	ΔH (J g^{-1})	ΔL (mm)	ΔM (%)
A	586.5	2.72	3.9
B	46.6	0.19	14.4

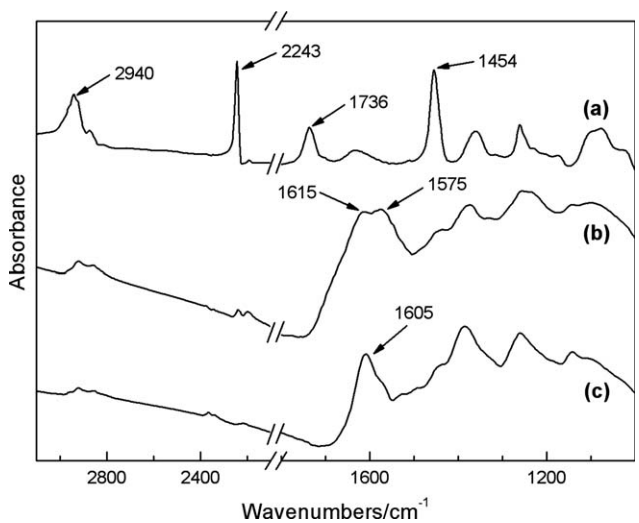

Figure 4 FT-IR spectra of PAN fibers: (a) PAN precursor; (b) after the first heating process; (c) after the second heating process.

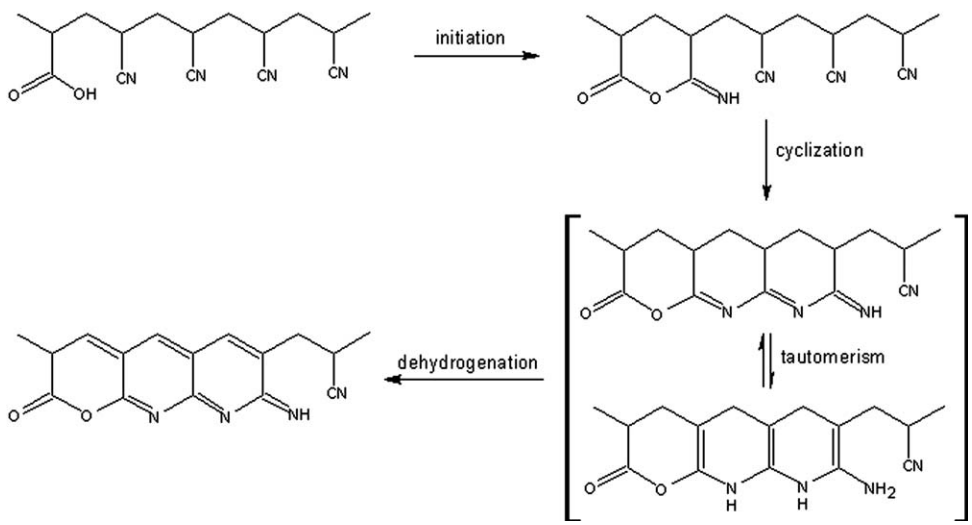

Figure 5 Structural evolution of PAN during thermal stabilization in inert gas.

is 0.19, that is to say around 80% of the nitrile groups are consumed during the first heating step. The existence of a small fraction of nitrile groups after very long reaction times at 238°C has also been observed by Beltz and Gustafson.[21] Figure 4(c) presents the spectrum of PAN sample after the second heating step. The band of nitrile groups almost completely disappeared. At the same time, a singlet band at 1605 cm^{-1} incorporating the 1615 cm^{-1} ($\nu_{C=N}$) and 1575 cm^{-1} ($\nu_{C=C}$) bands appeared, which might come from the formation of a fully conjugated structure due to dehydrogenation, as shown in Figure 5.

Thermal stabilization kinetics

From the results above, we interpreted the experimental data by distinguishing between cyclization and pyrolysis. In this part, the thermal stabilization kinetics of PAN fibers in an inert gas were investigated by conventional methods and a new method of regional kinetics (kinetics in different temperature regions) based on DSC, TMA, and TG data.

General kinetic study using DSC, TMA, and TG methods

The Kissinger[15] and Ozawa[16] methods were applied to determine the kinetic parameters of the thermal stabilization reactions. These two methods are frequently found in the literature because they only require a series of thermal behavior curves obtained at different heating rates. Table III shows the peak temperatures (T_p) of DSC, TMA, and TG curves for PAN under various heating rates in inert gas. With an increasing of heating rate (β), T_p presents a regular increase due to the lagging effect. T_p(TG) was higher than T_p(DSC) and T_p(TMA) at each heating rate, as mentioned above.

The mathematical expression of the Kissinger method is as follows[15]:

$$\ln\left(\frac{\beta}{T_p^2}\right) = \ln\left(\frac{AR}{E_a}\right) - \frac{E_a}{R}\frac{1}{T_p} \tag{2}$$

where T_p is the peak temperature; β is the heating rate; E_a is the apparent activation energy; A is the pre-exponential factor, and R is the mole gas constant. According to this equation, E_a and A can be calculated from the slope and the intercept, respectively, of a linear fitted plot of $\ln(\beta/T_p^2)$ against $1/T_p$.

The mathematical expression of the Ozawa method is as follows[16]:

$$\lg\beta = \lg\left(\frac{AE_a}{RG(\alpha)}\right) - 2.315 - 0.4567\frac{E_a}{R}\frac{1}{T_p} \tag{3}$$

where $G(\alpha)$ is a reaction function related to the mechanism. In the same method, E_a can be determined from the slope of a linear fitted plot of lgβ against $1/T_p$.

Figure 6 shows the kinetic fitting plots according to DSC, TMA, and TG curves by the Kissinger and

TABLE III
T_p of Different Thermal Behavior Curves of PAN Under Various Heating Rates

	T_p (°C)		
β (°C min^{-1})	DSC	TMA	TG
2	260	254	274
4	268	264	282
6	273	268	287
8	277	270	299
10	280	275	302

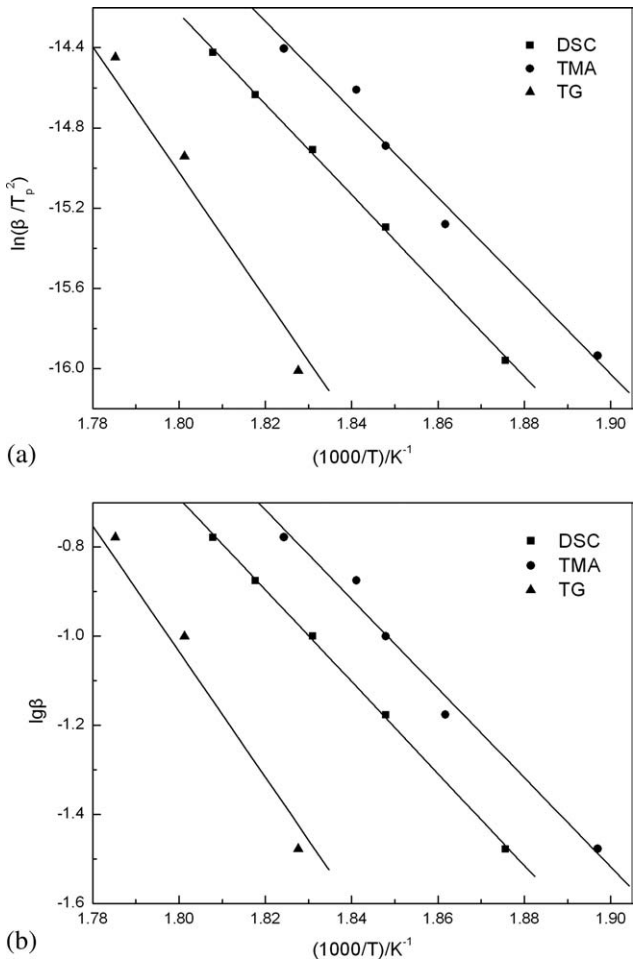

Figure 6 Linear fitting plots of PAN fibers according to different thermal behavior curves by the: (a) Kissinger method; (b) Ozawa method.

Ozawa methods. The linear dependence of each fitting plot is as expected, and the results of E_a and A are presented in Table IV. These two methods gave similar values for each E_a. The order of E_a values was: E_a(TMA) $<$ E_a(DSC) $<$ E_a(TG), where E_a(TMA) is close to E_a(DSC) and both are much lower than E_a(TG). This indicates that the energy barrier of pyrolytic reactions of PAN macromolecules is much higher than that of the cyclization reaction. The mechanism proposed above is reasonable when considered from the kinetics viewpoint: cyclization of nitrile groups occurs first and then pyrolytic reactions in PAN macromolecules take place when the temperature is sufficiently high.

Regional kinetic study using the DSC curve

Both the Kissinger and Ozawa methods are multiple rates methods, in which the kinetic parameters are determined in response to the peak temperatures of curves measured under different heating rates. If several reactions exist simultaneously in a thermal treatment process, the kinetic parameters calculated by these methods are for the overall reactions. In the case of the thermal stabilization of PAN fibers, it is necessary to apply several kinetic models to the different steps due to the coexistence of cyclization and pyrolytic reactions.

The Improved Coats-Redfern method[22–24] was employed to calculate the kinetic parameters of thermal stabilization reactions using the DSC curve within the temperature range from 216 to 307°C at 6°C min^{-1} heating rate. The mathematical expression of this method is as follows:

$$\ln \int_0^{\alpha} \frac{d\alpha}{(1-\alpha_i)^n T^2} = \ln\left(\frac{AR}{\beta E_\alpha}\right) - \frac{E_\alpha}{R}\frac{1}{T} \tag{4}$$

where T is the heating temperature, α_i is the conversion at temperature T, and n is the order of reaction. α_i is obtained from the relation:

$$\alpha_i = \frac{\Delta H_i}{\Delta H} \tag{5}$$

where ΔH_i is the cumulative enthalpy change before T and ΔH is the total enthalpy change. Y_i is assigned to the left side of eq. (4). The value of n is set and then E_a and A can be calculated from the slope and the intercept, respectively, from a linear fitted plot of Y_i against $1000/T$. The value of n can be determined when the linearity of the fitting plot is optimized.

Figure 7 shows the DSC kinetic curves of the improved Coats-Redfern method under different values of n from 0 to 2. When $n = 1$, the best linearity was obtained ($R = -0.9947$), so the thermal stabilization of PAN fibers in inert gas should occur as a first order reaction overall. The detail of the linear fit for $n = 1$ is shown in Figure 8. It was found that the curve could not be fitted as a straight line well, especially in the temperature region $1000/T < 1.86$ or $T > 263$°C. That is to say, during the pyrolytic reaction, when mass loss occurred, the first order mechanism is not suitable. Therefore, to describe the thermal stabilization of PAN fibers in inert gas precisely, kinetic models should be separated depending on different temperature regions.

Based on the results of characteristic temperatures, including T_i(DSC), T_i(TG), T_p(DSC), and T_f(DSC), the DSC curve was divided into three temperature regions: Region I is from 216 to 263°C, in which ΔH is dominated

TABLE IV
Kinetic Parameters in Figure 6

Methods	E_a (kJ mol^{-1})		A (1/s)
	Kissinger	Ozawa	Kissinger
DSC	188.2	187.6	7.451×10^{15}
TMA	182.7	182.2	3.269×10^{15}
TG	309.3	302.9	1.448×10^{27}

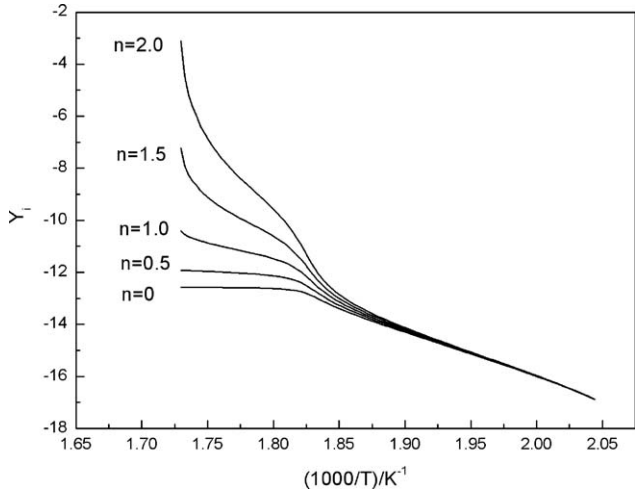

Figure 7 DSC kinetic curves by the Improved Coats-Redfern method ($\beta = 6°C\ min^{-1}$).

by cyclization of nitrile groups; Region II is from 263 to 273°C, in which multiple reactions exist. Pyrolysis takes place and affects ΔH; Region III is from 273 to 307°C. ΔH decreased rapidly after the peak temperature and the effect of pyrolysis became more significant.

Figure 9 presents the kinetic fitting plots according to the Improved Coats-Redfern method in the three regions described above. The linear dependence of each fitting plot is better than that of the overall fitting plot shown in Figure 8. The "Three Regions Kinetic Model" was obtained as follows:

$$\text{Region I}: \frac{d\alpha}{dT} = \frac{2.032 \times 10^{12}}{\beta} \exp\left(-\frac{151.0 \times 10^3}{RT}\right) \times (1-\alpha),\ T_i(\text{DSC}) < T < T_i(\text{TG}) \quad (6)$$

$$\text{Region II}: \frac{d\alpha}{dT} = \frac{2.962 \times 10^{12}}{\beta} \exp\left(-\frac{153.6 \times 10^3}{RT}\right) \times (1-\alpha)^{-0.5},\ T_i(\text{TG}) < \text{T} < T_p(\text{DSC}) \quad (7)$$

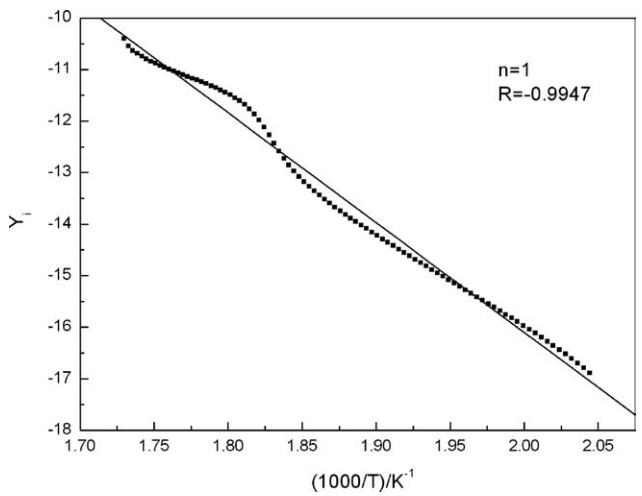

Figure 8 Linear fitting plot of $n = 1$ in Figure 7.

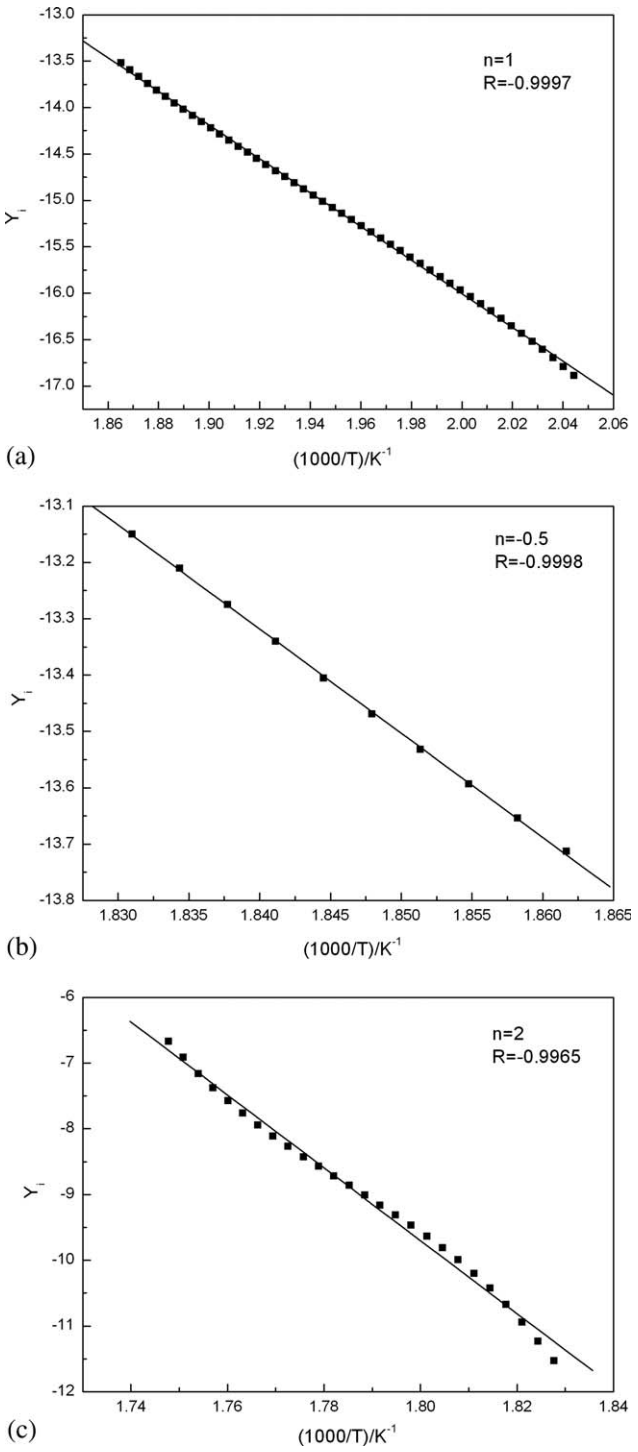

Figure 9 Fitting plots of regional kinetic models for: (a) Region I; (b) Region II; (c) Region III.

$$\text{Region III}: \frac{d\alpha}{dT} = \frac{1.891 \times 10^{45}}{\beta} \exp\left(-\frac{483.9 \times 10^3}{RT}\right) \times (1-\alpha)^2,\ T_p(\text{DSC}) < T < T_f(\text{DSC}) \quad (8)$$

The deviation of the calculated apparent activation energy in eqs. (6)–(8) was ~ 2%, which may have been caused by systematic errors such as apparatus

error. Equations (6)–(8) indicate that only Region I can be described in a first order kinetic scheme. In Regions II and III, reactions become much more complicated. Pyrolytic reactions occur and play an important role in the change of enthalpy. The models therefore deviate from a first order kinetic equation.

A typical comparison between the experimental and simulation profiles in a plot of $d\alpha/dT$ versus α is shown in Figure 10, where $d\alpha/dT$ is the conversion rate. It is shown that the simulation curve and the experimental curve are matched quite well, so this model is feasible for describing the thermal stabilization process of PAN at a given heating rate. The model is therefore useful for predicting the thermal stabilization profile at a given heating rate. As is shown in Figure 11, the predicted profiles conform to the experimental data within error limits at 2 and 10°C min^{-1}.

CONCLUSIONS

Thermal behavior and kinetics during the thermal stabilization process of PAN fibers from 40 to 400°C in inert gas were studied. The comparison of DSC, TMA, and TG showed that complex reactions occurred and the thermal behaviors show correspondence to different reaction evolution processes. Based on a detailed analysis, the mechanism for thermal stabilization of PAN fibers in inert gas was proposed. FT-IR spectra implied that most of the nitrile groups were consumed at 240°C in inert gas and an imine-enamine tautomeric structure was formed. This structure was converted to a conjugated structure when the treatment temperature increased to 400°C.

Kinetic results developed by the Kissinger and Ozawa methods showed that TMA method was also suitable for kinetic study of thermal stabilization of PAN fibers and provided further evidence for the proposed mechanism. The preliminary kinetic results deduced by the Improved Coats-Redfern method using the DSC curve indicated that thermal stabilization of PAN fibers in inert gas was a first order reaction overall. However, some parts of the curve could not be fitted with reasonable linearity. The "Three Regions Kinetic Model" was therefore proposed. This model could describe the thermal stabilization process much better than an overall kinetic model.

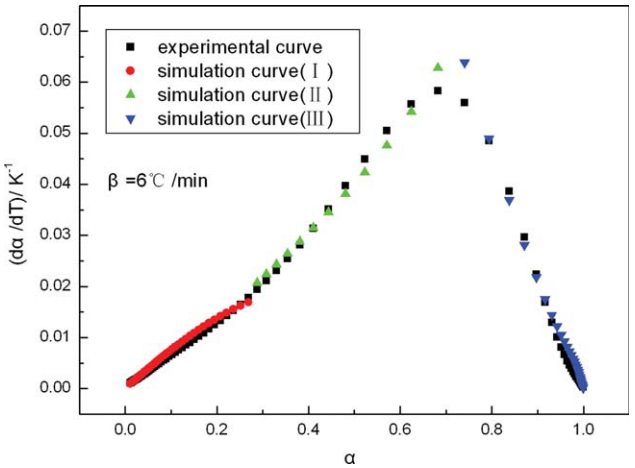

Figure 10 Verified profiles of the "Three Regions Kinetic Model." [Color figure can be viewed in the online issue, which is available at wileyonlinelibrary.com.]

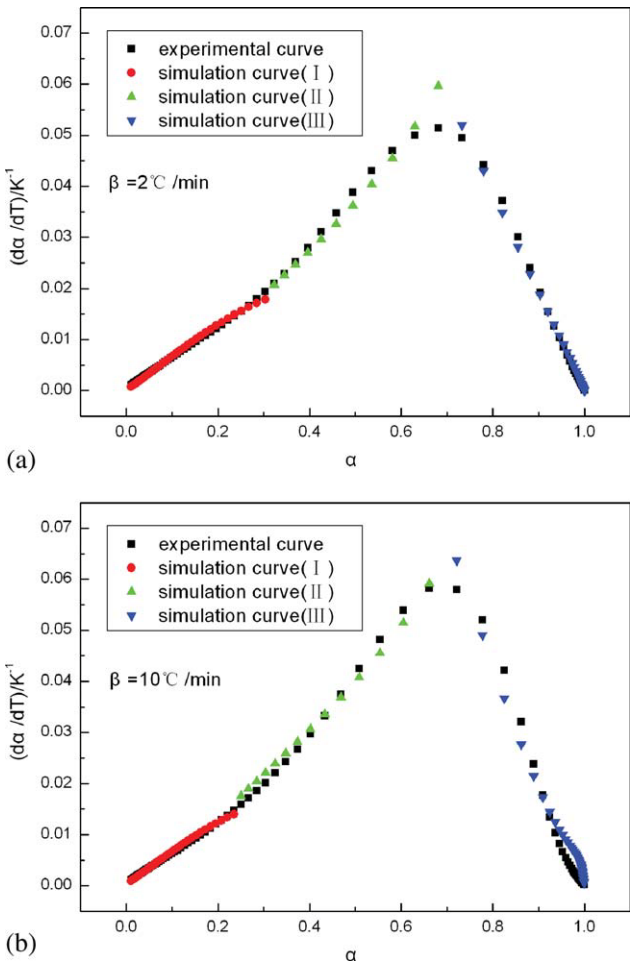

Figure 11 Predicted profiles of the "Three Regions Kinetic Model" for: (a) β = 2°C min^{-1}; (b) β = 10°C min^{-1}.[Color figure can be viewed in the online issue, which is available at wileyonlinelibrary.com.]

References

1. Watt, W.; Johnson, W. Nature 1975, 257, 210.
2. Sivy, G. T.; Gordon, B.; Coleman, M. M. Carbon 1983, 21, 573.
3. Coleman, M. M.; Sivy, G. T.; Painter, P. C.; Snyder, R. W.; Gordon, B. Carbon 1983, 21, 255.
4. Fitzer, E.; Frohs, W.; Heine, M. Carbon 1986, 24, 387.
5. Bajaj, P.; Sreekumar, T. V.; Sen, K. Polymer 2001, 42, 1707.
6. Cui, C. S.; Yu, L.; Wang, C. G. J Appl Polym Sci 2010, 117, 1596.
7. Chen, H.; Qu, R. J.; Wang, Q.; Liang, Y.; Wang, C. G. J Appl Polym Sci 2005, 98, 1708.

8. Liu, J.; Zhou, P. X.; Zhang, L. F.; Ma, Z. K.; Liang, J. Y.; Fong, H. Carbon 2009, 47, 1087.
9. Zhang, W. X.; Liu, J.; Wu, G. Carbon 2003, 41, 2805.
10. Fitzer, E.; Muller, D. J Carbon 1975, 13, 63.
11. Collins, G. L.; Thomas, N. W.; Williams, G. E. Carbon 1988, 26, 671.
12. Hay, J. N. J Polym Sci Polym Chem 1968, 6, 2127.
13. Devasia, R.; Reghunadhan Nair, C. P.; Sivadasan, P.; Katherine, B. K.; Ninan, K. N. J Appl Polym Sci 2003, 88, 915.
14. Ouyang, Q.; Lu, C.; Wang, H. J.; Li, K. X. Polym Degrad Stab 2008, 93, 1415.
15. Kissinger, H. E. Anal Chem 1957, 29, 1702.
16. Ozawa T. Bull Chem Soc Jpn 1965, 38, 1881.
17. Noh, I.; Yu, H. J Polym Sci Polym Lett 1966, 4, 721.
18. Morita, K.; Miyachi, H.; Hiramatsu, T. Carbon 1981, 19, 1.
19. Kakida, H.; Tashiro, K.; Kobayashi, M. Polym J 1996, 28, 30.
20. Kakida, H.; Tashiro, K.; Polym J 1998, 30, 463.
21. Beltz, L. A.; Gustafson, R. R. Carbon 1996, 34, 561.
22. Coats, A. W.; Redfern, J. P. Nature 1964, 201, 68.
23. Eftimic, E.; Segal, E. Thermochim Acta 1987, 111, 359.
24. Ning, B. K.; Yang, Z. Q.; Liu, R. Chin J Expl Prop 2000, 1, 65.